NASA TECHNICAL REPORT

NASA TR R-266

NASA TR R-266

c.1

FATIGUE LIFE UNDER RANDOM LOADING FOR SEVERAL POWER SPECTRAL SHAPES

by Sherman A. Clevenson and Roy Steiner

Langley Research Center
Langley Station, Hampton, Va.

NATIONAL AERONAUTICS AND SPACE ADMINISTRATION • WASHINGTON, D. C. • SEPTEMBER 1967

FATIGUE LIFE UNDER RANDOM LOADING FOR SEVERAL POWER SPECTRAL SHAPES

By Sherman A. Clevenson and Roy Steiner

Langley Research Center
Langley Station, Hampton, Va.

NATIONAL AERONAUTICS AND SPACE ADMINISTRATION

For sale by the Clearinghouse for Federal Scientific and Technical Information
Springfield, Virginia 22151 – CFSTI price $3.00

FATIGUE LIFE UNDER RANDOM LOADING FOR SEVERAL POWER SPECTRAL SHAPES

By Sherman A. Clevenson and Roy Steiner
Langley Research Center

SUMMARY

Each of a number of aluminum-alloy test specimens was loaded by random forces at a constant root-mean-square stress level until rupture occurred. The forces were statistically stationary and Gaussian with a zero mean value. The fatigue life (to rupture) was determined for various values of the following statistical parameters: (a) root-mean-square nominal applied stress, (b) power spectral shape, (c) mean number of zero crossings per unit time, and (d) mean number of peak loads per unit time. The power spectra were varied over a passband of frequency for three spectral shapes either by holding the power constant with frequency or by varying it either directly or inversely proportional to the square of the frequency.

The results indicate that the fatigue life was determined principally by the root-mean-square nominal applied stress level. The effects of spectral shape, average number of zero crossings, and average number of peak loads were insignificant in the ranges investigated. The fatigue life, based on the number of effective cycles, of the specimens under random loading was lower by at least an order of magnitude at all stress levels than that of the specimens loaded sinusoidally. A linear cumulative damage theory overestimated the fatigue life, especially at low stress levels. The fracture characteristics of the specimens which failed under random loading were similar to those which failed under sinusoidal loads.

INTRODUCTION

Fatigue failures have plagued designers and operators of dynamic structures for many years. The fatigue failure problem for randomly loaded structures, such as aircraft, is becoming more frequent with the trend toward more efficient use of metal. At the same time, the procedures for predicting the fatigue life of these structures are unsatisfactory; consequently the operators are forced to inspect and repair the structures to provide a satisfactory service life.

The present prediction methods evolved from those based on the earliest experiences with fatigue failures in rotating and reciprocating machine elements. These elements were subjected to periodic loads having almost constant amplitude and it followed that fatigue test specimens could be loaded sinusoidally at constant amplitude to provide information for fatigue life prediction. This approach subsequently was extended for the prediction of fatigue life of randomly loaded structures by introducing the concept of cumulative damage (refs. 1 and 2). In this concept the continuous random load is assumed to be represented by groups of sinusoidal loadings having different amplitudes, the amplitudes within a group being constant. The total fatigue life of the structure is assumed to be allocated among the groups in proportion to the number of cycles in each group and on the basis of the life at the various load levels as determined from the sinusoidal fatigue tests.

Because of the poor predictions of fatigue life for randomly loaded structures based on test data for sinusoidal loadings, an investigation was undertaken to obtain some additional test data. In the study, aluminum-alloy specimens were tested to failure (rupture) under random loading in order to determine whether the fatigue life can be consistently related to the statistical parameters that describe the loads. The random loading processes chosen were the same as those which describe short samples of natural phenomena such as atmospheric turbulence, buffet velocities, and acoustical noise. This process possesses stationary and Gaussian statistical characteristics and may be represented by a power spectral density function. Several spectral shapes and variations in statistical parameters were used in the tests. The results are compared with those from sinusoidal loadings and with the predictions from the linear cumulative damage theory.

SYMBOLS

Dimensional values are given both in U.S. Customary Units and in the International System of Units (SI). Factors relating the two systems are given in reference 3.

K — arbitrary constant

M_n — the nth moment of power spectrum, $\int_0^\infty \omega^n \phi(\omega) d\omega$

M_0 — mean-square loading, $\int_0^\infty \phi(\omega) d\omega$ or σ^2

$M_2 = \int_0^\infty \omega^2 \phi(\omega) d\omega$

$M_4 = \int_0^\infty \omega^4 \phi(\omega) d\omega$

N_f average number of cycles to rupture

N_p average number of stress maximums per second, $\frac{1}{2\pi}\left(\frac{M_4}{M_2}\right)^{1/2}$

$N_{p,s}$ average number of peaks above a given stress level per second

N_0 average number of crossings of a zero mean with a positive slope per second, $\frac{1}{2\pi}\left(\frac{M_2}{M_0}\right)^{1/2}$

n any even order of the moment, 0, 2, 4, . . .

S nominal stress, kips per square inch (meganewtons per square meter)

S_p nominal peak stress, kips per square inch (meganewtons per square meter)

t_f time to rupture, seconds

σ^2 mean-square loading

$\phi(\omega)$ power spectral density as a function of frequency; loading spectrum

ω angular frequency, radians per second

Subscripts:

av average

rms root mean square

STATISTICAL PARAMETERS AND SPECTRA

For the class of random processes used in the fatigue tests (stationary and Gaussian), the statistical properties can be defined from the power spectrum of the loads if the mean load is zero or if a known mean is subtracted from the time function. A series of statistical parameters can be obtained from the power spectrum by use of the equation (from refs. 4 and 5)

$$M_n = \int_0^\infty \omega^n \phi(\omega) d\omega \tag{1}$$

where $n = 0, 2, 4, \ldots$. For $n = 0$, M_n is the variance or the mean-square value about the mean and is a measure of the intensity of the random phenomenon; that is,

$$M_0 = \sigma^2 = \int_0^\infty \phi(\omega) d\omega \tag{2}$$

For $n = 2$, M_n yields information concerning N_0, the average number of zero crossings with positive slope per second; that is,

$$N_0 = \frac{1}{2\pi}\left(\frac{M_2}{M_0}\right)^{1/2} = \frac{1}{2\pi}\left(\frac{\int_0^\infty \omega^2 \phi(\omega) d\omega}{\int_0^\infty \phi(\omega) d\omega}\right)^{1/2} \tag{3}$$

For $n = 4$, M_n yields information concerning N_p, the average number of maximums per second; that is,

$$N_p = \frac{1}{2\pi}\left(\frac{M_4}{M_2}\right)^{1/2} = \frac{1}{2\pi}\left(\frac{\int_0^\infty \omega^4 \phi(\omega) d\omega}{\int_0^\infty \omega^2 \phi(\omega) d\omega}\right)^{1/2} \tag{4}$$

There are, of course, additional moments based on larger values of n, but for most applications they have not appeared to be practical or necessary. These parameters (eqs. (2), (3), and (4)) lend themselves to a presentation of fatigue test results in a manner similar to the S–N (stress against number of cycles) curves associated with sinusoidal loadings. The parameter σ, the root-mean-square value, is the counterpart of S and is equally applicable to sine functions and to random time functions. Either of the parameters N_0 or N_p may be used with the test time to rupture to provide a measure of the life in average numbers of cycles or peaks $\left(N_0 t_f \text{ or } N_p t_f = N_f\right)$.

There is a wide variation in possible loads or stress spectra ranging from white noise (spectra with constant power for an infinite frequency range) to narrow-band spectra

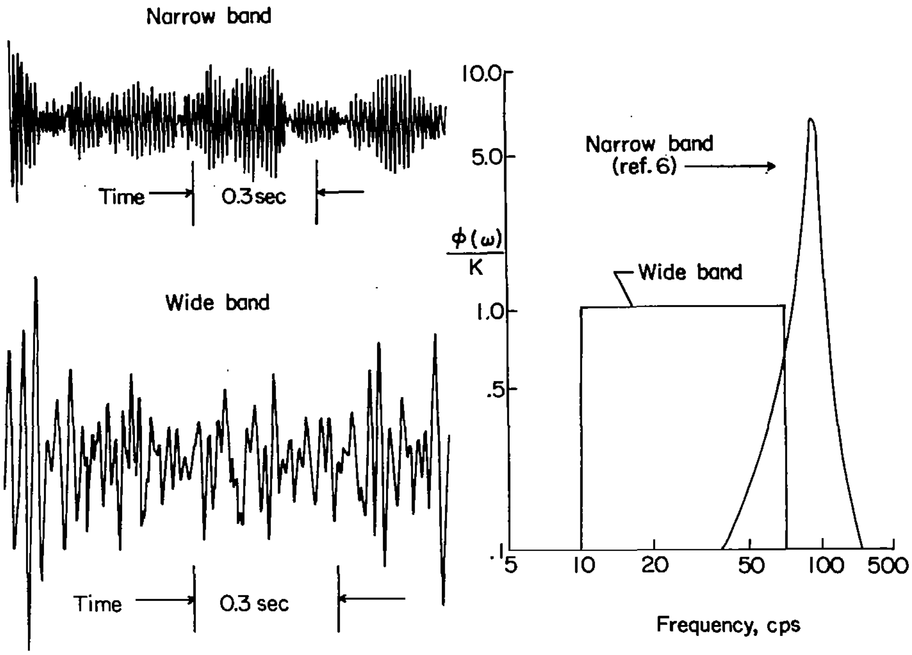

Figure 1.- Contrast between wide-band frequency and narrow-band frequency random excitation. The power spectral densities have the same root-mean-square value.

(spectra with a large portion of the power concentrated near a single frequency). In figure 1, both the time history of a narrow-band (ref. 6) and a wide-band frequency function and the corresponding spectra are shown for equal root-mean-square values. The narrow-band time histories give the appearance of containing one frequency whose amplitude varies relatively slowly with time. This type of random loading occurs on a resonant system when subjected to a random (both frequency and amplitude) input. (See ref. 7.) The spectrum indicates a peak in power at some center frequency with a rapid fall-off on each side. The wide-band time history appears to be a random combination of both amplitudes and frequencies over a finite range. The power spectrum shown for the wide-band time history is idealized and indicates relatively constant power within the frequency range indicated.

In the present study three different spectral shapes were selected both to cover a wide range of shapes and to retain simplicity of investigation. The spectra (shown in fig. 2) varied over a passband of frequency as follows:

$$\phi(\omega) = K_1\omega^{-2}$$

$$\phi(\omega) = K_2\omega^{0}$$

$$\phi(\omega) = K_3\omega^{2}$$

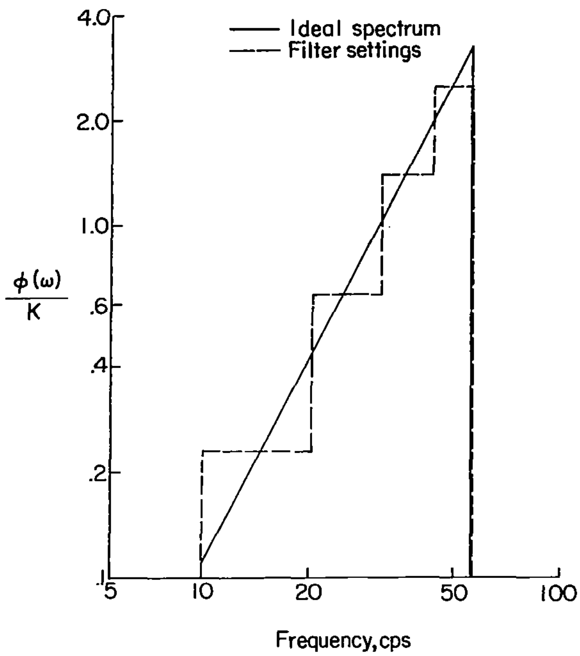

(a) Case 1: $\Phi(\omega) = K_3\omega^2$, $N_0 = 43$, and $N_p/N_0 = 1.12$.

Figure 2.- Selected spectra for fatigue testing.

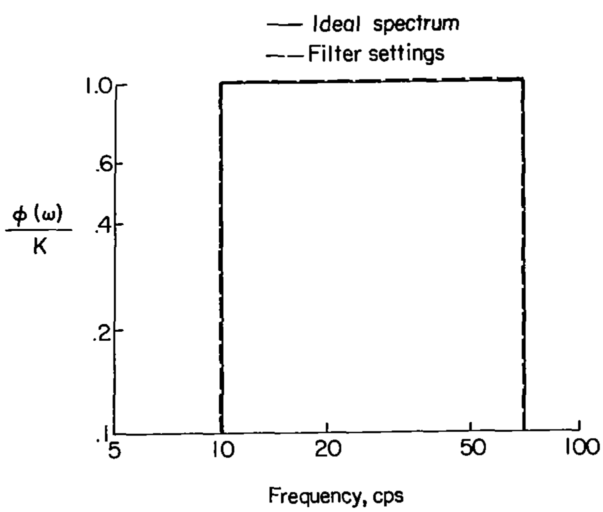

(b) Case 1: $\Phi(\omega) = K_2\omega^0$, $N_0 = 43$, and $N_p/N_0 = 1.10$.

Figure 2.- Continued.

These spectra are not necessarily representative, individually, of actual loadings on structures in service. Neither are they representative of the narrow-band spectrum commonly used for random fatigue testing.

TEST PROCEDURE

Test Program

In order to understand the results of testing with random loading and to establish an appropriate base for comparison, the test program was divided into three phases. The first phase consisted of conventional static tensile tests to rupture of a number of specimens to obtain both a load-deflection relationship and the ultimate strength of the material. In the second phase fatigue failure data were obtained under various sinusoidal loadings at low frequencies (10, 20, and 40 cps) to establish an S-N relation in the usual manner. In the third phase fatigue failure data were obtained under random loading.

In the random load tests, each test specimen was loaded at a constant root-mean-square level until rupture occurred. Results from a series of specimens established the variation of fatigue life $\left(N_0 t_f \text{ or } N_p t_f\right)$ with root-mean-square load for a given combination of spectral shape $\phi(\omega)$, average number of zero crossings per unit time N_0, and average number of peak loads per unit time N_p. From a number of test series, the effects of the individual quantities $\phi(\omega)$, N_0, and N_p were determined by varying one parameter while the rest were held constant. Spectral shape variation is designated case 1. Cases 2 and 4

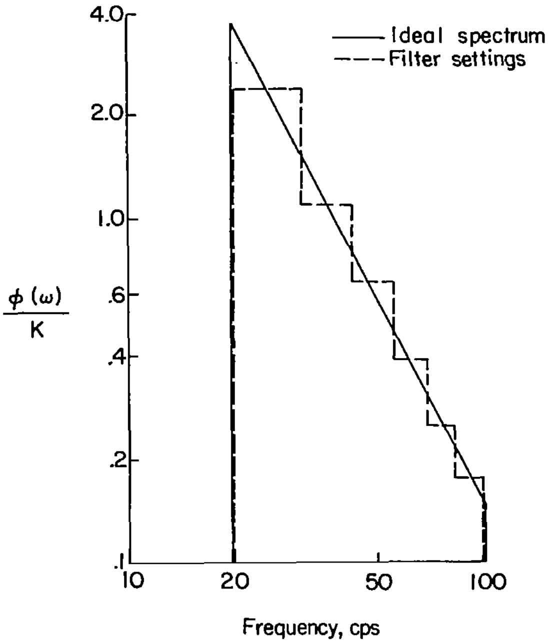

(c) Case 1: $\Phi(\omega) = K_1\omega^{-2}$, $N_0 = 44$, and $N_p/N_0 = 1.21$.

Figure 2.- Continued.

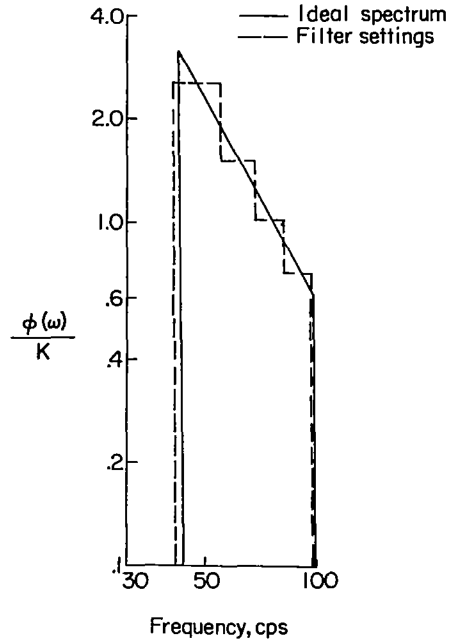

(d) Case 2: $\Phi(\omega) = K_1\omega^{-2}$, $N_0 = 67$, and $N_p/N_0 = 1.23$.

Figure 2.- Continued.

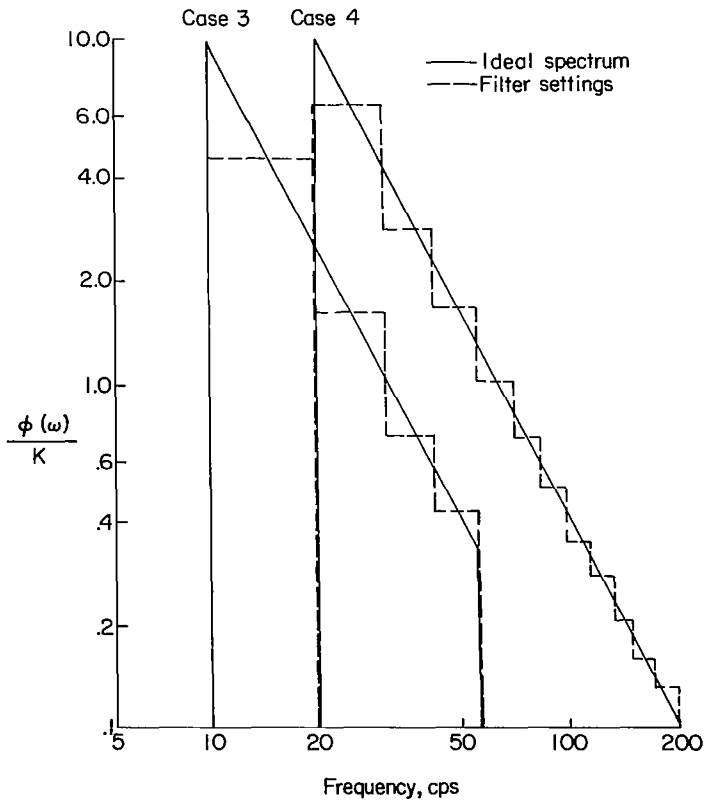

(e) Case 3: $\Phi(\omega) = K_1\omega^{-2}$, $N_0 = 43$, and $N_p/N_0 = 1.57$;
Case 4: $\Phi(\omega) = K_1\omega^{-2}$, $N_0 = 54$, and $N_p/N_0 = 1.34$.

Figure 2.- Concluded.

identify changes in N_0; N_p/N_0 was varied in case 3. The ranges of the parameters were limited by the frequency range (10 to 200 cps) of the loading apparatus. The test spectra were chosen to provide the largest changes in N_0 and N_p consistent with these requirements and limitations. The ranges of the parameters are given in table I.

Test Specimens

Approximately 100 test specimens were made of 2024-T4 aluminum-alloy round stock from the same mill run and each had a machined test section 0.5000 inch (1.27 cm) in diameter to give a theoretical stress concentration of 2.2. The radius of curvature at the test section was 0.0625 inch (0.159 cm). These specimens were tested to rupture in this study. A photograph of a typical specimen is shown in figure 3.

Test Setups

Two different test setups were required to conduct the three phases of the test program. A static tensile testing machine was used for the determination of the ultimate strength of the specimen and a 30 000-pound (134 kN) complex electromagnetic shaker utilizing automatic sinusoidal and random controls was used in the fatigue (vibration) tests as indicated in figure 4(a). The test specimen was located between the 30 000-pound (134 kN) force electromagnetic shaker and a 50 000-pound (222 kN) load cell which was rigidly attached to the backstop. The load cell, specimen, and shaker system had a flat frequency response to over 200 cps, which was greater than the range of test frequencies.

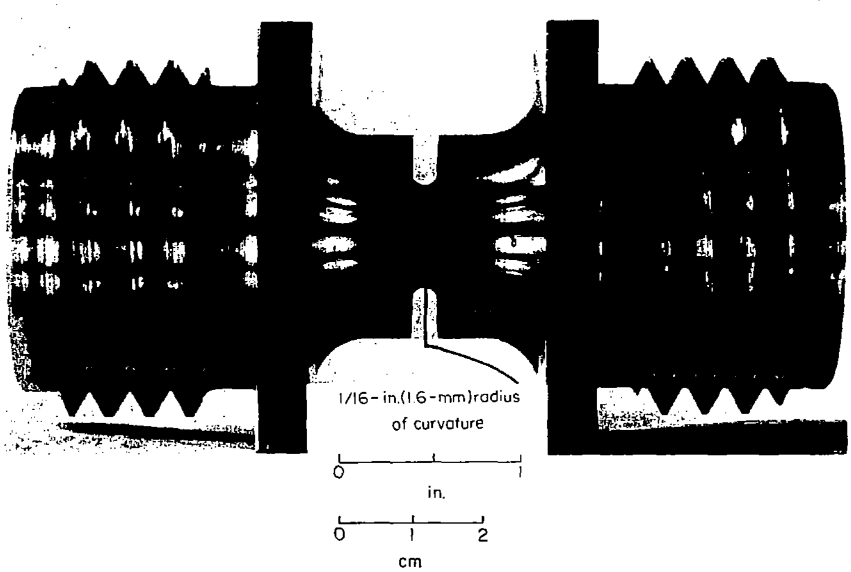

Figure 3.- Fatigue test specimen. L-67-1004

For this frequency range, thermal stresses were considered to be unimportant. To obtain consistent results, great care was required in the installation of the specimens to insure both that no internal stresses were preset in the specimens and that they were correctly alined.

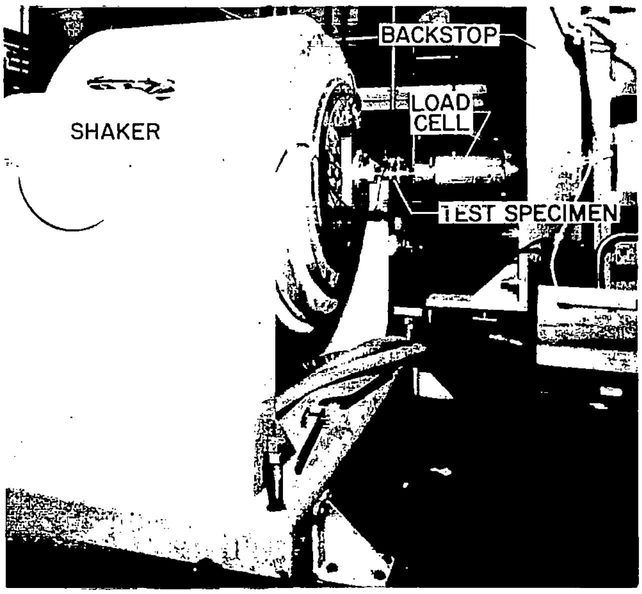

(a) Complex vibration loading system. L-67-1005

Figure 4.- Test setup.

A closeup photograph of the test specimen and a break-circuit mechanism is shown in figure 4(b). The mechanism consisted of a preloaded cantilever spring which closed the electrical circuit to the exciter by a microswitch. When the specimen failed, spring action opened the exciter circuit and thus immediately discontinued the force (within 1 to 2 cycles).

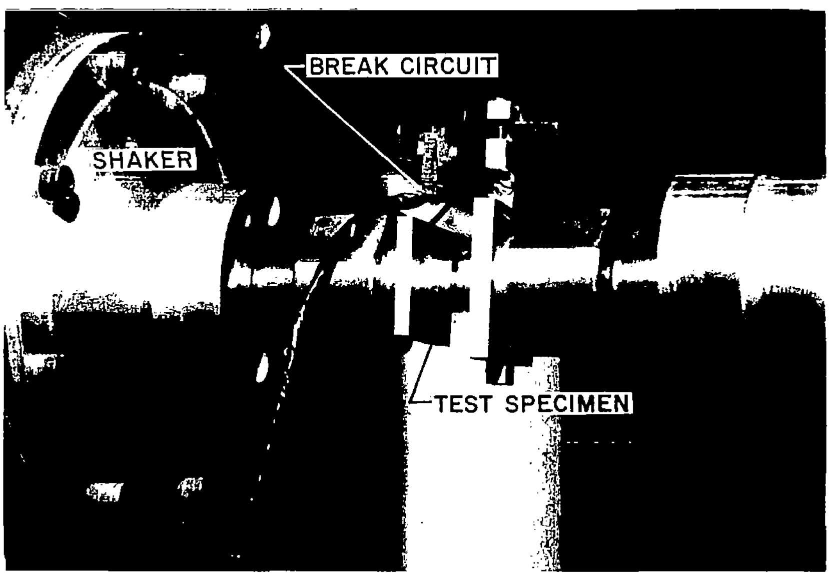

(b) Break-circuit mechanism. L-67-1006

Figure 4.- Concluded.

A block diagram of the test setup for fatigue tests is shown in figure 5. The signal originated from a random noise generator. The shaping of the test spectrum was accomplished with an automatic spectral density analyzer-equalizer (servo-signal shaper) utilizing narrow-band filters. (See figs. 2(a) to 2(e).) The servo-signal shaper was used to filter the signal from the random noise generator to provide the desired spectrum. The signal passed through a low-pass filter and the break circuit and was amplified to drive a 30 000-pound

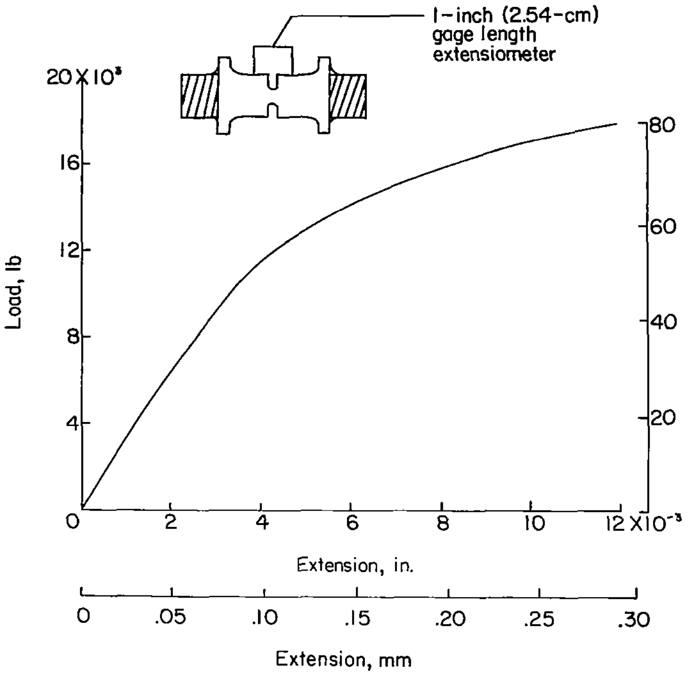

Figure 6.- Elongation of test specimen with load. Ultimate load, 18 830 pounds (84 kN).

Sinusoidal Loading

An S-N curve established by the test results for the sinusoidal loading condition (table II) is shown in figure 7 where the maximum nominal stress level is presented as a function of number of cycles to rupture. The test frequency was 10, 20, or 40 cps as indicated in table II. A solid curve was faired through the experimental data. In each case, the stress was plotted as the peak stress. This faired curve has the form

$$N_pS^b = c$$

where b and c are constants. On log-log paper, the curve is a

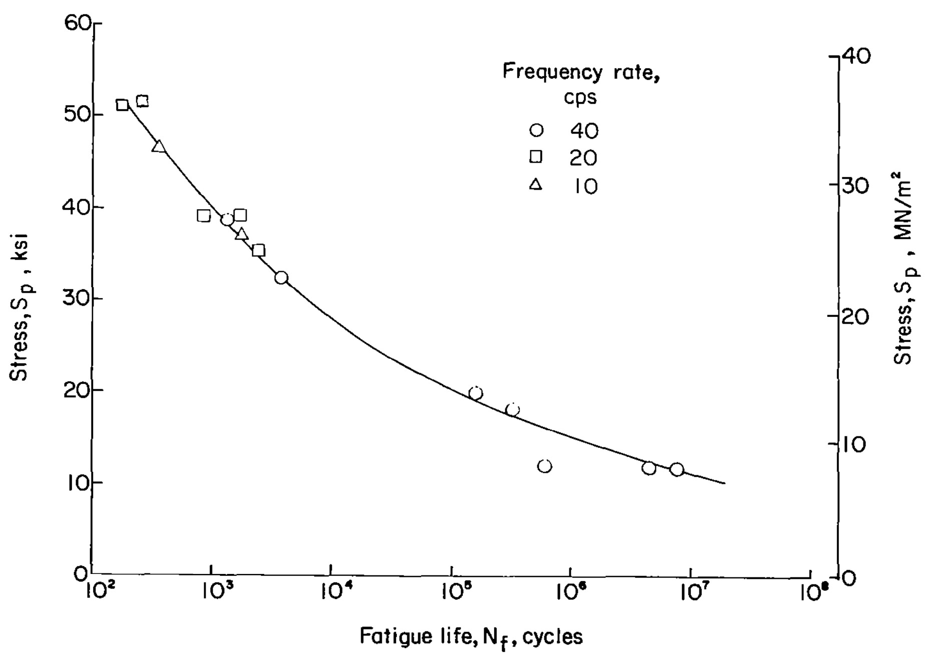

Figure 7.- Fatigue life of aluminum-alloy specimens for sinusoidal loading.

straight line with slope -b. The constants for the sinusoidal loading were determined as $b = 7.14$ and $c = 6.1 \times 10^{35}$.

The effect of frequency of loading in the range investigated was apparently small. At a peak stress level of approximately 38 ksi (261.9 MN/m^2) specimens were failed at frequency rates of 10, 20, and 40 cps. The number of cycles to failure, as indicated by the data points in figure 7, was fairly consistent and independent of loading frequency.

Random Loading

The results, including the statistical parameters, for the random loadings are summarized in table III.

Statistical characteristics.- To obtain various statistical characteristics, sample time histories were recorded during the tests and analyzed to verify that the root-mean-square stress value was at the desired level, that the loading function possessed the desired qualities of stationary and normal distributions, and that the average number of zero crossings and of peaks agreed with the theoretical values.

Root-mean-square levels were measured continuously during each run and, by observing constancy of the levels, the stationary process was verified.

Normality of the loading process was checked by comparing plots of data samples on a normal probability scale with the ideal straight-line relation between cumulative probability and stress level. The probability was determined from stress readings at equal time intervals which were small compared with the period of the highest frequency component. A representative plot is given in figure 8. The fit of the straight line to the measured data indicates that the process is indeed essentially Gaussian.

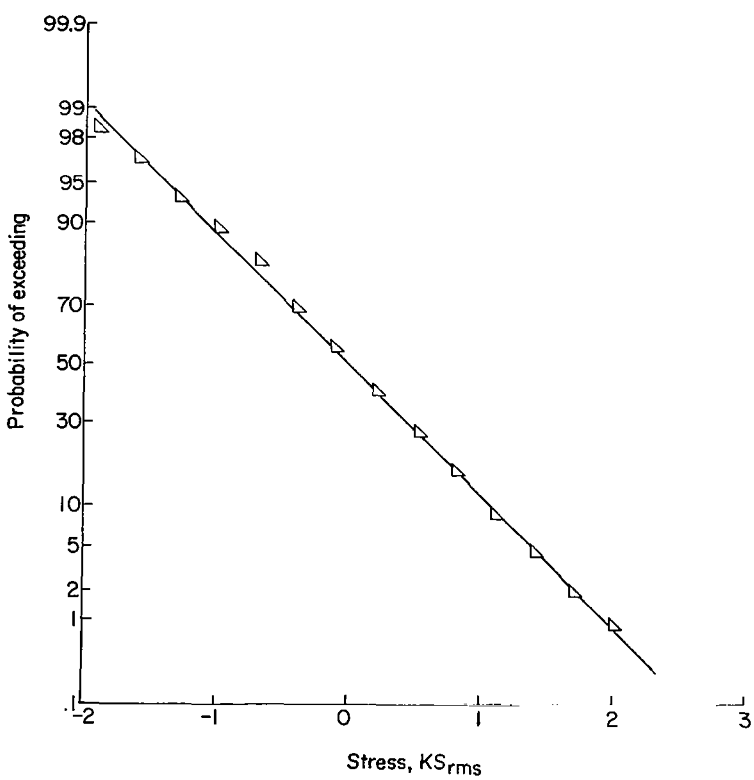

Figure 8.- Distribution of amplitude based on readings at equal time intervals.

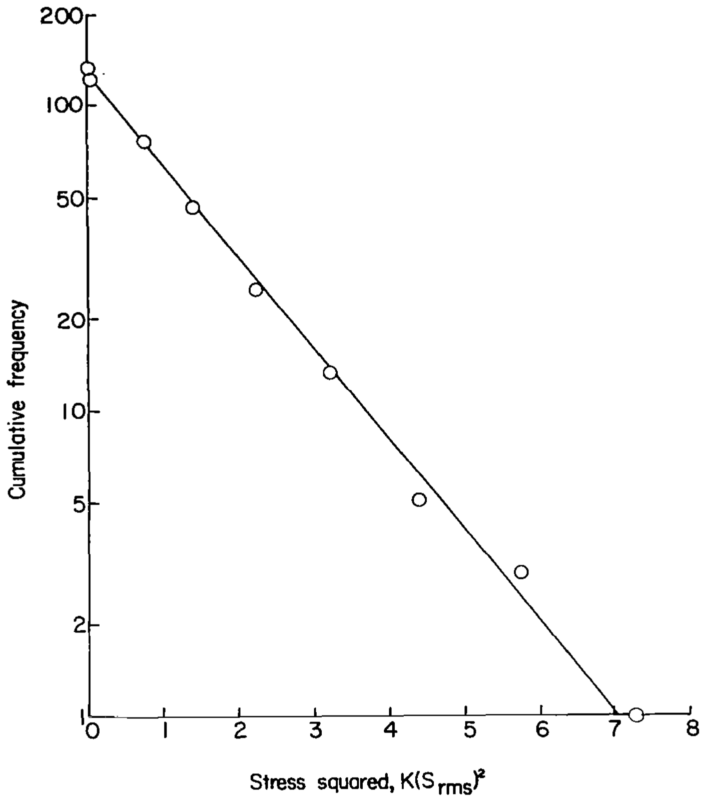

Figure 9.- Cumulative frequency of peak stresses that exceed given levels as a function of stress level squared.

A further indication of normality of the loading process was obtained from the approximate equation for the average true number of maximum peaks exceeding given stress levels for a Gaussian process. The equation is

$$N_{p,s} = N_0 e^{-\frac{S^2}{2\sigma^2}}$$

This expression is exact for the average number of crossings of level S with a positive slope. The approximation for the peaks is satisfactory for values of S/σ greater than about unity. A plot of the square of the stress level as a function of $\log N_{p,s}$ is a straight line having a slope equal to $1/2\sigma^2$. In figure 9 the normality of the loading process is corroborated on this basis by the agreement between data from the tests and the ideal straight line. The average number of zero crossings and of peaks are verified by direct counting.

In the interest of economy, it was desirable to limit analysis of the random time functions to the smallest practical sample size; from trial analyses of sample times in multiples of 1 second it was determined that at least a 3-second sample was required for statistical reliability and, therefore, a 3-second sample was used for analyses.

Effect of spectral shape and statistical parameters.- The effects of spectral shape on the fatigue life are shown in figure 10. The fatigue life as defined by the number of cycles (total number of zero crossings with positive slope $N_0 t_f$) until failure is shown as a function of the root-mean-square stress for all three spectra of case 1. For this case, the ratio of N_p/N_0 was essentially constant at about 1.15, N_0 was approximately 43 positive crossings per second, and the root-mean-square stress levels ranged from 3.56 to 24.95 ksi (24.53 to 173 MN/m^2). A dashed curve represents a fairing through each set of data and indicates essentially no difference in the fatigue lives of these specimens when randomly loaded as specified in the aforementioned three spectra. It is

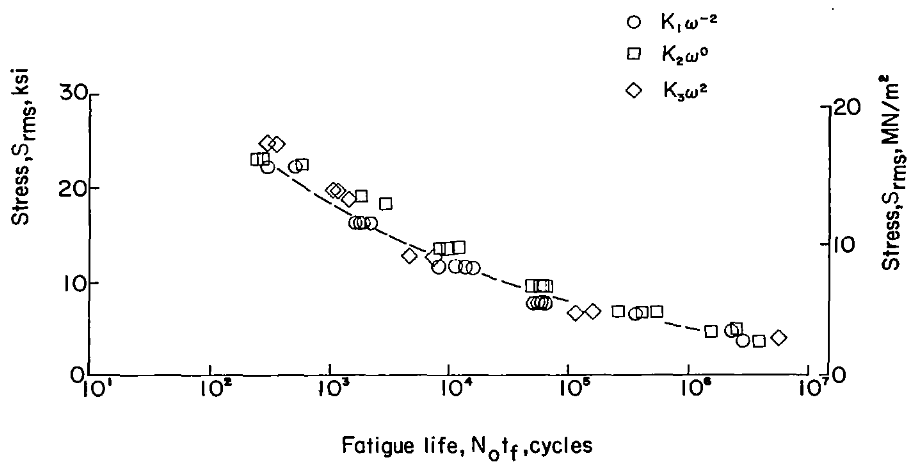

Figure 10.- Fatigue life of 2024-T4 aluminum-alloy specimens for case 1. $N_p/N_0 \approx 1.15$; $N_0 \approx 43$.

noteworthy that, like the S-N curve from the sinusoidal load tests, this curve has the form

$$N_p S^b = c$$

where b and c are constants. These constants (based on root-mean-square stress, not on peak stress) were experimentally determined as $b = 5.26$ and $c = 1.8 \times 10^{25}$ for the random tests as compared with 7.14 and 9.75×10^{22}, respectively, for the sinusoidal tests.

The effect of N_0 is shown in figure 11 where the data of case 2, $N_0 = 67$, may be compared with the data of case 1, $N_0 = 44$, for $\phi(\omega) = K_1\omega^{-2}$. The ratio N_p/N_0 was

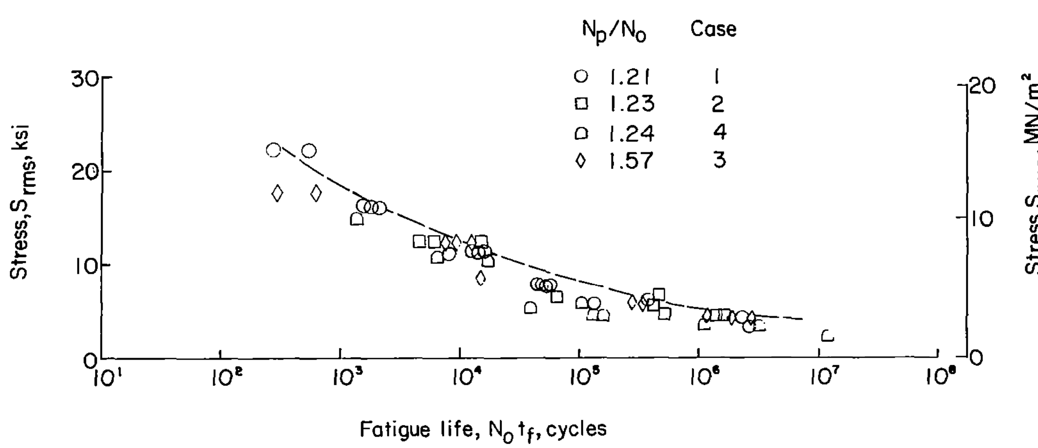

Figure 11.- Fatigue life based on number of zero crossings for $\Phi(\omega) = K_1\omega^{-2}$.

approximately 1.22. The data appear to be overlapping; hence, the effect of N_0 on the fatigue life is considered to be negligible.

Also in figure 11, the effect of N_p/N_0 may be observed by comparing case 1, $N_p/N_0 = 1.21$, with case 3, $N_p/N_0 = 1.57$. In each case, N_0 is approximately 43. Actually all data could be used in the comparisons since it has been indicated previously that N_0 had a negligible effect on the fatigue life. The dashed curve was taken from figure 10 for reference. All four sets of data, especially those for cases 1 and 3, appear to be overlapping. The figure indicates, therefore, that the effect of N_p/N_0 is negligible in the range investigated.

The data from figure 11 were replotted in figure 12 as stress against fatigue life as defined by the total number of maximums $\left(N_p t_f\right)$. The dashed curve taken from figure 10 has again been shown for reference. It may be noted that the data fall on either side of the curve and also intermix for the various ratios of N_p/N_0. It is indicated, therefore, that the representation of fatigue life may be based equally well on the number of cycles or on the number of peaks when specimens are subjected to random loadings. However the curves based on N_0 and N_p are not theoretically interchangeable. Although tests were not made for the other spectra, similar results would be expected.

Comparison of fatigue lives for random and sinusoidal loadings.- Figure 13 summarizes the data of figures 10 and 7 to provide a comparison of the data on the fatigue lives for sinusoidal and random loading. The peak stresses of figure 7 have been converted to root-mean-square stresses. For the higher stress levels, it appears that the fatigue life of the randomly loaded specimens was one order of magnitude less than that of the sinusoidally loaded specimens. At the lower stress levels, the difference is even greater.

Comparisons with linear cumulative damage estimates.- Fatigue life under random loading was estimated by a procedure based on the Palmgren-Miner hypothesis described

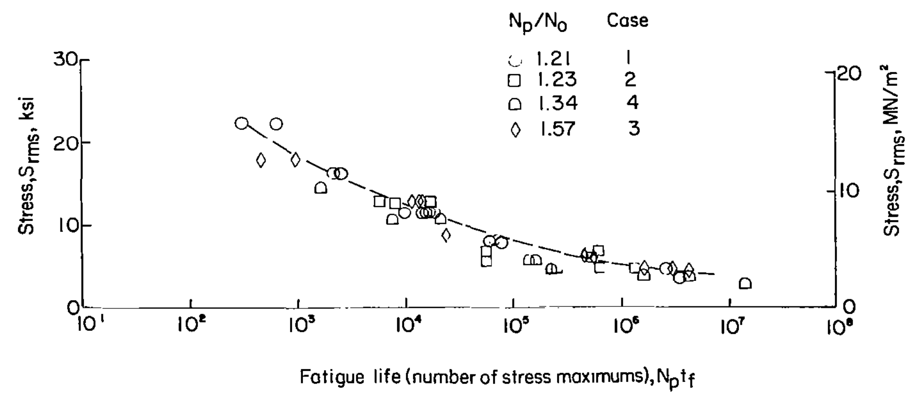

Figure 12.- Fatigue life based on number of stress maximums for $\Phi(\omega) = K_1\omega^{-2}$.

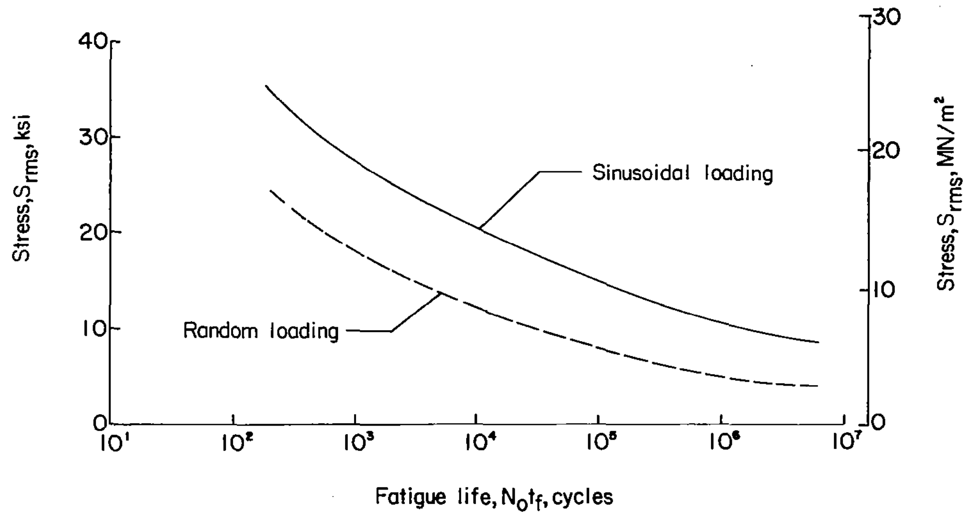

Figure 13.- Comparison of fatigue lives for random and sinusoidal loading.

in references 1 and 2. In this hypothesis, fatigue life is defined as the number of cycles to crack initiation. It is common practice, however, to apply the hypothesis to fatigue life in terms of cycles to rupture and this application is used herein.

The average numbers of cycles (or peaks) in a given stress increment above various stress levels, as required in the Palmgren-Miner hypothesis, were established from cumulative frequency curves for a given root-mean-square stress such as that in figure 9. The method used is described in reference 8. The fatigue life at each of several root-mean-square stress levels was determined from this information together with the S-N curve in figure 7.

The ratio of the actual fatigue life to that predicted by the cumulative damage method is presented in figure 14 for several root-mean-square stresses. It is apparent that for the low stress values the fatigue life in terms of rupture is greatly overestimated. For the 7.50-ksi (51.7 MN/m^2) stress, for example, the actual fatigue life was only one-tenth of the predicted amount. For the higher stress levels, fatigue life is predicted more accurately, but the stress levels are approaching unrealistically high working values.

It is generally acknowledged that the low-intensity loads are of great importance in fatigue. The results of these tests, therefore, indicate that the cumulative damage method of fatigue life estimation should be used with caution.

Failure modes.- Photographs made of the failed areas of the test specimens showed, in general, the expected characteristics of structural tension and fatigue failures. Figure 15 shows the cross section of a specimen failed in tension (static load) and a series of areas of specimens failed at various root-mean-square stress levels. The

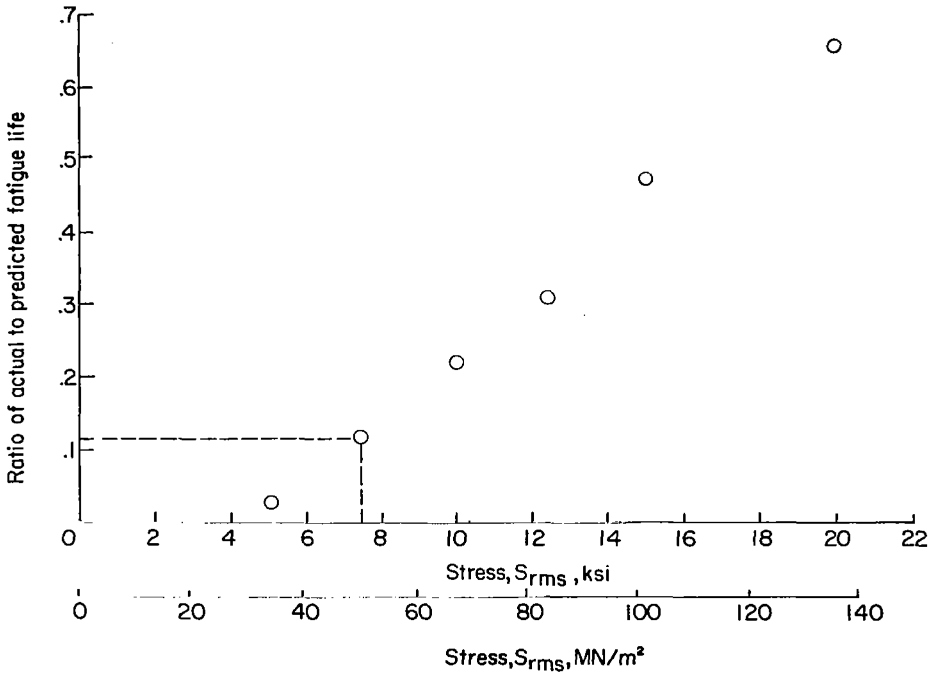

Figure 14.- Indication of applicability of the linear cumulative damage hypothesis to prediction of fatigue life.

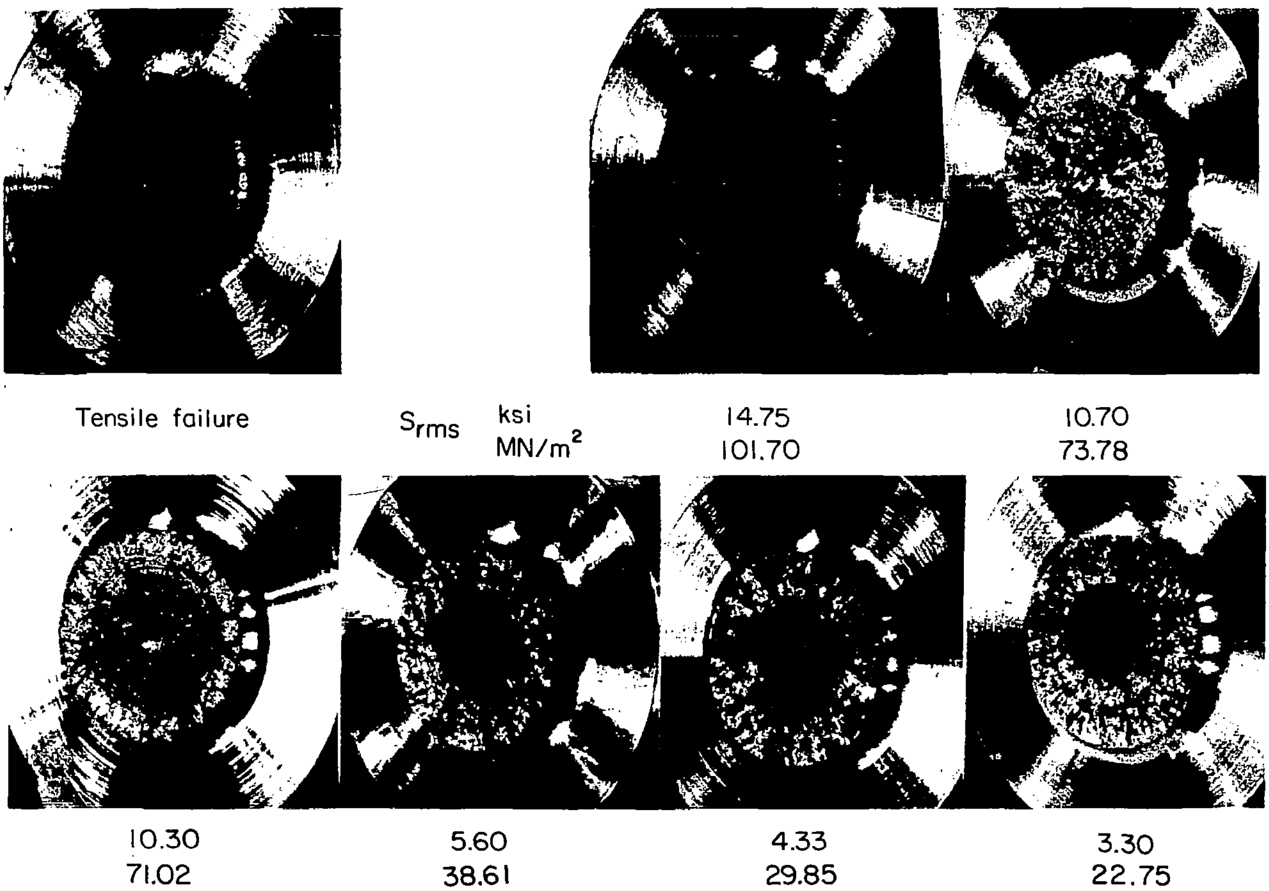

L-67-1007

Figure 15.- Samples of tensile and fatigue failures at various root-mean-square stress levels. $N_p/N_0 = 1.34$; $\Phi(\omega) = K_1\omega^{-2}$.

levels shown are 14.75, 10.70, 10.30, 5.60, 4.33, and 3.30 ksi (101.70, 73.78, 71.02, 38.61, 29.85, and 22.75 MN/m^2). The other conditions remained constant: $\phi(\omega) = K_1\omega^{-2}$, $N_p/N_0 = 1.34$, and $N_0 = 54$.

It may be noted that the static tensile failure had relatively uniform characteristics over the entire area of fracture. The failed specimen at the root-mean-square stress level of 14.75 ksi (101.70 MN/m^2) also appears to have a relatively uniform area of fracture. However, as the root-mean-square stress level is decreased, the area of fracture progressively changes. At a root-mean-square stress level of 3.30 ksi (22.75 MN/m^2), it may be noted that an inner circle consisting of approximately one-third of the test area diameter still retains the characteristic appearance of the specimen failed in tension. The outer circular area has many radial lines (fatigue cracks) appearing to start at the outer edge of the specimen. Thus, it may be concluded that the entire fracture may be due to different kinds of failure. Similar results were obtained on the sinusoidally loaded specimens.

CONCLUDING REMARKS

A study of the fatigue life of aluminum-alloy specimens under stationary and Gaussian random loadings having a zero mean value has been conducted. The random loadings were described by power spectral densities of the form $\phi(\omega) = K_1\omega^{-2}$, $K_2\omega^0$, and $K_3\omega^2$ in the frequency range 10 to 200 cps, where K is an arbitrary constant and ω is the angular frequency. The results for the random loadings indicate that the fatigue life was determined principally by the root-mean-square nominal applied stress level. The effects of spectral shape, average number of zero crossings, and average number of peak loads were insignificant in the range investigated. The average number of zero crossings with positive slope per second was varied from 43 to 67. The ratio of number of peaks to number of zero crossings varied from 1.10 to 1.57. The fatigue life, based on the number of effective cycles, of the specimens under random loading was lower by at least an order of magnitude at all stress levels than that of the specimens loaded sinusoidally. A linear cumulative damage theory overestimated the fatigue life for random loadings, especially at low stress levels. The fracture characteristics of the specimens which failed under random loading were similar to those which failed under sinusoidal loading.

Langley Research Center,
National Aeronautics and Space Administration,
Langley Station, Hampton, Va., February 24, 1967,
124-08-05-02-23.

REFERENCES

1. Palmgren, Arvid: Die Lebensdauer von Kugellagern. (The Lifetime of Ball Bearings.) Z.V.D.I., Bd. 68, Nr. 14, Apr. 1924, pp. 339-341.
2. Miner, Milton A.: Cumulative Damage in Fatigue. J. Appl. Mech., vol. 12, no. 3, Sept. 1945, pp. A-159 – A-164.
3. Mechtly, E. A.: The International System of Units – Physical Constants and Conversion Factors. NASA SP-7012, 1964.
4. Blackman, R. B.; and Tukey, J. W.: The Measurement of Power Spectra. Dover Publ., Inc., 1959.
5. Press, Harry; Meadows, May T.; and Hadlock, Ivan: A Reevaluation of Data on Atmospheric Turbulence and Airplane Gust Loads for Application in Spectral Calculations. NACA Rept. 1272, 1956. (Supersedes NACA TN 3362 by Press, Meadows, and Hadlock and TN 3540 by Press and Meadows.)
6. Phillips, Edward P.: Fatigue of René 41 under Constant- and Random-Amplitude Loading at Room and Elevated Temperatures. NASA TN D-3075, 1965.
7. Crandall, Stephen H.; and Mark, William D.: Random Vibration in Mechanical Systems. Academic Press, Inc., 1963.
8. Whaley, Richard E.: Fatigue Investigation of Full-Scale Transport-Airplane Wings – Variable-Amplitude Tests With a Gust-Loads Spectrum. NACA TN 4132, 1957.

TABLE I.- TEST CONDITIONS

Power spectra of loading, $\phi(\omega)$	Average number of zero crossings per second, N_0	Average ratio of peaks to zero crossings, $\left(N_p/N_0\right)_{av}$	Range of rms stress levels, S_{rms}		Remarks
			ksi	MN/m^2	
Case 1					
$K_1\omega^{-2}$	44	1.21	3.570 to 22.140	24.61 to 152.60	Effect of spectra
$K_2\omega^{0}$	43	1.10	3.950 to 22.950	27.22 to 172	Effect of spectra
$K_3\omega^{2}$	43	1.12	3.560 to 22.900	24.55 to 157.9	Effect of spectra
Case 2					
$K_1\omega^{-2}$	67	1.23	4.580 to 12.700	31.58 to 87.6	Effect of N_0
Case 3					
$K_1\omega^{-2}$	43	1.57	4.280 to 17.800	29.5 to 122.6	Effect of N_p/N_0
Case 4					
$K_1\omega^{-2}$	54	1.34	2.540 to 14.750	17.51 to 101.7	Effect of N_0

TABLE II.- FATIGUE DATA FOR SINUSOIDAL LOADING

Stress, S_p		Stress, S_{rms}		Frequency, cps	Time, t_f, seconds	Number of cycles, $N_0 \times t_f$
ksi	MN/m^2	ksi	MN/m^2			
11.8	81.4	8.35	57.6	40	202 200	8 088 000
11.8	81.4	8.35	57.6	40	113 700	4 545 000
11.8	81.4	8.35	57.6	40	15 000	600 000
18.1	124.9	12.8	88.3	40	8 220	329 000
20.1	138.5	14.2	98.0	40	4 620	184 000
32.5	224.0	23.0	158.5	40	97.80	3 920
35.0	241.2	24.8	171.0	20	114.00	2 290
37.1	255.8	26.2	180.6	10	160.20	1 600
38.6	266.1	27.3	189.1	40	33.18	1 329
39.1	269.6	27.7	192.0	20	75.42	1 510
39.1	269.6	27.7	192.0	20	41.52	831
46.3	318.1	32.8	226.1	10	28.02	280
51.9	357.9	36.6	252.1	20	8.46	171
52.3	360.5	37.0	255.0	20	13.92	244

TABLE III.- FATIGUE DATA FOR RANDOM LOADING

Stress, S_{rms}		N_0	N_p/N_0	Time, t_f, seconds	Cycles, $N_0 \times t_f$	Peaks, $N_p \times t_f$
ksi	MN/m^2					
$K_3\omega^2$ spectrum – case 1						
3.56	24.5	42	1.17	93 360	3.93×10^6	4.60×10^6
4.74	32.7	41	1.13	61 860	2.54×10^6	2.89×10^6
4.74	32.7	42	1.15	32 340	1.36×10^6	1.56×10^6
6.42	44.2	42	1.10	11 400	4.79×10^5	5.27×10^5
6.42	44.2	46	1.04	5 490	2.53×10^5	2.63×10^5
6.42	44.2	42	1.03	9 660	4.05×10^5	4.17×10^5
9.17	63.2	42	1.06	1 440	6.05×10^4	6.42×10^4
9.17	63.2	42	1.03	1 200	5.04×10^4	5.20×10^4
9.17	63.2	42	1.10	1 410	5.92×10^4	6.54×10^4
13.50	93.1	43	1.06	259.8	1.12×10^4	1.19×10^4
13.50	93.1	42	1.10	225.0	9.45×10^3	1.04×10^4
13.50	93.1	44	1.12	198.0	8.80×10^3	9.86×10^3
18.10	124.8	46	1.01	64.98	2.98×10^3	3.02×10^3
18.74	129.2	44	1.22	30.54	1.83×10^3	2.23×10^3
22.00	151.7	60	1.20	90.0	5.40×10^3	6.48×10^3
22.90	158.0	36	1.30	7.98	2.87×10^2	3.73×10^2
22.90	158.0	39	1.20	6.48	2.53×10^2	3.04×10^2
$K_2\omega^0$ spectrum – case 1						
3.95	27.2	45	1.10	128 880	5.80×10^6	6.34×10^6
6.40	44.1	45	1.13	3 540	1.59×10^5	1.79×10^5
6.40	44.1	42	1.15	2 700	1.13×10^5	1.30×10^5
8.91	61.4	43	1.15	1 302	5.60×10^4	6.44×10^4
12.60	86.9	46	1.09	122.4	5.63×10^3	6.14×10^3
12.60	86.9	42	1.12	204.0	8.56×10^3	9.70×10^3
18.85	130.0	47	1.04	26.76	1.26×10^3	1.31×10^3
19.50	134.5	43	1.16	24.00	1.01×10^3	1.17×10^3
19.50	134.5	50	1.08	21.00	1.05×10^3	1.13×10^3
24.95	172.0	43	1.08	8.22	3.53×10^2	3.81×10^2
24.95	172.0	46	1.13	6.78	2.98×10^2	3.37×10^2

TABLE III.- FATIGUE DATA FOR RANDOM LOADING – Continued

Stress, S_{rms}		N_0	N_p/N_0	Time, t_f, seconds	Cycles, $N_0 \times t_f$	Peaks, $N_p \times t_f$
ksi	MN/m^2					
$K_1\omega^{-2}$ spectrum – case 1						
3.57	24.6	46	1.20	65 580	2.87×10^6	3.45×10^6
4.47	30.8	43	1.22	51 660	2.22×10^6	2.71×10^6
6.12	42.2	44	1.16	8 850	3.90×10^5	4.53×10^5
7.90	54.4	42	1.19	1 332	5.59×10^4	6.66×10^4
7.90	54.4	43	1.25	1 320	5.67×10^4	7.09×10^4
7.90	54.4	40	1.28	1 530	6.12×10^4	7.84×10^4
11.20	77.2	42	1.24	334.8	1.41×10^4	1.75×10^4
11.20	77.2	43	1.28	319.8	1.38×10^4	1.78×10^4
11.20	77.2	43	1.20	295.8	1.27×10^4	1.53×10^4
11.20	77.2	43	1.20	183.6	7.90×10^3	9.49×10^3
16.04	110.5	45	1.19	44.70	2.03×10^3	2.42×10^3
16.04	110.5	44	1.25	42.00	1.85×10^3	2.31×10^3
16.04	110.5	42	1.17	40.02	1.68×10^3	1.97×10^3
22.14	152.6	45	1.22	11.58	5.22×10^2	6.37×10^2
22.14	152.6	52	1.10	6.48	2.80×10^2	3.08×10^2
$K_1\omega^{-2}$ spectrum – case 2						
4.58	31.6	63	1.29	19 080	1.20×10^6	1.55×10^6
4.58	31.6	129	1.22	9 120	1.18×10^6	1.44×10^6
4.58	31.6	64	1.17	8 040	5.15×10^5	6.03×10^5
6.00	41.4	66	1.16	6 300	4.16×10^5	4.83×10^5
6.36	43.8	65	1.27	7 020	4.56×10^5	5.79×10^5
6.36	43.8	70	1.14	9 660	6.78×10^4	7.74×10^4
12.70	87.6	66	1.26	202.2	1.33×10^4	1.68×10^4
12.70	87.6	81	1.33	75.0	6.07×10^3	8.08×10^3
12.70	87.6	63	1.27	73.2	4.58×10^3	5.70×10^3

TABLE III.- FATIGUE DATA FOR RANDOM LOADING – Concluded

Stress, S_{rms}		N_0	N_p/N_0	Time, t_f, seconds	Cycles, $N_0 \times t_f$	Peaks, $N_p \times t_f$
ksi	MN/m^2					
$K_1\omega^{-2}$ spectrum – case 3						
4.28	29.5	56	1.58	51 180	2.87×10^6	4.54×10^6
4.28	29.5	50	1.55	39 300	1.97×10^6	3.06×10^6
4.28	29.5	43	1.59	25 200	1.08×10^6	1.72×10^6
6.00	41.4	42	1.65	7 980	3.36×10^5	5.55×10^5
6.00	41.4	51	1.59	5 640	2.88×10^5	4.58×10^5
8.65	59.6	33	1.68	420.0	1.41×10^4	2.36×10^4
12.20	84.2	44	1.55	225.0	9.90×10^3	1.53×10^4
12.20	84.2	56	1.39	193.2	1.08×10^4	1.50×10^4
12.20	84.2	44	1.64	165.0	7.26×10^3	1.19×10^4
17.80	122.8	31	1.61	20.40	6.20×10^2	9.96×10^2
17.80	122.8	27	1.49	11.40	3.02×10^2	4.50×10^2
$K_1\omega^{-2}$ spectrum – case 4						
2.54	17.5	60	1.18	182 460	1.10×10^7	1.29×10^7
3.30	22.7	46	1.32	67 080	3.09×10^6	4.08×10^6
3.30	22.7	48	1.42	22 080	1.07×10^6	1.51×10^6
4.33	29.8	56	1.47	2 460	1.38×10^5	2.03×10^5
4.33	29.8	57	1.63	2 340	1.33×10^5	2.17×10^5
5.60	38.6	56	1.22	2 340	1.31×10^5	1.60×10^5
5.60	38.6	50	1.32	2 160	1.08×10^5	1.43×10^5
5.60	38.6	47	1.46	840	3.95×10^4	5.77×10^4
10.30	71.0	60	1.18	289.8	1.74×10^4	2.05×10^4
10.70	73.8	58	1.21	108.0	6.26×10^3	7.59×10^3
14.75	101.4	53	1.37	22.02	1.17×10^3	1.60×10^3

NASA-Langley, 1967 —— 32 L-5079